Ultramicroscopy 111 (2011) 1328–1337

Contents lists available at ScienceDirect

Ultramicroscopy

journal homepage: www.elsevier.com/locate/ultramic

Dark-field electron holography for the measurement of geometric phase

M.J. Hÿtch *, F. Houdellier, F. Hüe [1], E. Snoeck

CEMES-CNRS and Université de Toulouse, 29 rue Jeanne Marvig, F-31055 Toulouse, France

ARTICLE INFO

Article history:
Received 28 July 2010
Received in revised form
19 April 2011
Accepted 24 April 2011
Available online 30 April 2011

Keywords:
Electron holography
Dark-field electron holography
Geometric phase
Strain

ABSTRACT

The genesis, theoretical basis and practical application of the new electron holographic dark-field technique for mapping strain in nanostructures are presented. The development places geometric phase within a unified theoretical framework for phase measurements by electron holography. The total phase of the transmitted and diffracted beams is described as a sum of four contributions: crystalline, electrostatic, magnetic and geometric. Each contribution is outlined briefly and leads to the proposal to measure geometric phase by dark-field electron holography (DFEH). The experimental conditions, phase reconstruction and analysis are detailed for off-axis electron holography using examples from the field of semiconductors. A method for correcting for thickness variations will be proposed and demonstrated using the phase from the corresponding bright-field electron hologram.

1. Introduction

Electron holography has been used for an ever widening range of applications ever since its invention by Gabor [1]. In his original conception, the measurement of the phase of the wave front would allow the determination of the aberrations of the optical system, and hence their elimination. This objective has been pursued and perfected in the field of high-resolution off-axis electron holography [2,3]. In the medium-resolution variety, understood as the measurement of the phase of the transmitted beam with respect to the vacuum, electron holography has been used to confirm the existence of the phase change due to the magnetic vector potential [4]. The local in-plane projection of the magnetic field can thus be determined [5], which has led to the development of the methodology for the quantitative study of magnetic fields at the nanoscale [6,7] and direct comparisons with micromagnetics modelling [8,9]. Similarly, the phase changes due to slowly varying electrostatic fields have been studied by medium-resolution holography, from the measurement of mean inner potentials of materials [10], to the potential drop across p–n junctions [11], the mapping of dopant concentrations in semiconductors [12], and the electric fields around emitting tips [13]. Indeed, the combination of electron holography and electron tomography heralds an era of many new results [14,15]. The current state of the art can be found in a number of reviews [16,17,18] and the recent Hannes Lichte 65th birthday issue of Ultramicroscopy [19].

However, electron holography is not limited to the measurement of these phases, as we will show. Geometric phase can also be measured and quantified by electron holography [20,21] using the dark-field electron holography (DFEH) configuration [22]. The technique has opened up a new range of applications for measuring strain in crystalline materials, notably in the field of semiconductor devices and thin films [23–27].

Geometric phase had previously been measured primarily by high-resolution electron microscopy (HRTEM) [28]. Its influence on conventional diffraction contrast has been recognised since almost the origins of electron microscopy [29] and from a more formal point of view, it is related to Berry phase, also known as geometric phase [30]. In electron microscopy, however, geometric phase usually refers to the variation of the phase across the wave front and not in the direction of propagation. In retrospect, it is natural to think that geometric phase could be measured directly by electron holography.

Our first attempt to measure geometric phase with electron holography was to analyse high-resolution electron holograms (HREH) in a similar way to HRTEM images [31]. Unfortunately the benefits are limited with respect to the latter technique and led to the idea of measuring the geometric phase directly from the diffracted beam [20]. The dark-field off-axis electron holography configuration we used was, in fact, a rediscovery of previous work by Hanszen, which had been left largely forgotten [22]. Whilst off-axis electron holography is a particularly efficient and accepted means to determine phases, there is no reason that other holography schemes should not be explored, such as by using in-line holography in a follow up to our experiments [32]. Indeed, there are more than twenty holographic configurations, which can be pursued [33].

* Corresponding author.
E-mail address: hytch@cemes.fr (M.J. Hÿtch).
[1] Present address: University of Cambridge, Department of Materials Science, Pembroke Street, Cambridge, UK.

0304-3991/$ - see front matter © 2011 Elsevier B.V. All rights reserved.
doi:10.1016/j.ultramic.2011.04.008

The aim of this paper is to outline the theory that led to the idea of dark-field holography, to describe the experimental setup and conditions, and to identify the systematic and random errors, which can influence the accuracy and precision of the strain measurements. The theoretical development will lead to a proposal for correcting systematic errors due to thickness variations. Examples will be given to illustrate both the method and the application of corrections. Whilst the experiments are all carried out in the off-axis mode, the theory and analysis are general to the other configurations of electron holography. Indeed, the benefits of off-axis with respect to in-line holography are expected to be the same as for other applications of medium-resolution holography and are not specific to dark-field experiments. For a direct comparison, see for example Ref. [34].

2. Electron holography

The different configurations for off-axis electron holography that will be discussed in this paper are shown schematically in Fig. 1. Plane-wave illumination is formed from the highly localised source and directed towards the object. In the conventional setup (Fig. 1a) part of the electron wave passes through the specimen and the other part through the vacuum. These two beams are deflected with the aid of a tuneable electrostatic biprism, so that they overlap to create an interference pattern on the screen. The electron hologram then encodes the phase difference between the electron paths through the vacuum and through the specimen. These phase shifts can be due to the presence of magnetic fields, electrostatic fields (including the crystalline atomic potential) and, as we will show, displacement fields.

The electron wave passing to the left, ψ_L, and right, ψ_R, of the biprism will interfere to produce holographic fringes of intensity $|\psi|^2$:

$$\psi_L = a_L e^{i\phi_L} e^{2\pi i \vec{k}_L \cdot \vec{r}}$$

$$\psi_R = a_R e^{i\phi_R} e^{2\pi i \vec{k}_R \cdot \vec{r}}$$

$$|\psi|^2 = |\psi_L + \psi_R|^2 = a_R^2 + a_L^2 + 2a_R a_L \cos\{2\pi \vec{q}_c \cdot \vec{r} + \phi_{RL}\} \tag{1}$$

where $\vec{q}_c = \vec{k}_R - \vec{k}_L$ is known as the carrier frequency, and $\phi_{RL} = \phi_R - \phi_L$, the phase difference. The phase of the hologram can be extracted by one of the phase retrieval methods, such as the Fourier transform method, assuming a particular carrier frequency.

Eq. (1) is only valid for a single electron and needs to be integrated over the many electrons forming the image during the exposure time. The finite size of the electron source will limit the spatial coherence of the illumination and hence diminish the fringe contrast. Instabilities of the biprism (position and potential) will likewise reduce the fringe contrast as will the modulation transfer function (MTF) of the detector. All these factors will reduce the precision of the phase measurements.

2.1. Phase contributions

In most descriptions of medium-resolution electron holography, only the phase change of the transmitted beam is considered. Here, we will interest ourselves with the phase changes of both the transmitted and the diffracted beams created by a crystalline specimen. In addition, we will consider that the crystal is non-uniform; though departures from the norm will be treated as a perturbation. The wave function of the fast electron at the exit surface the crystal, $\psi(\mathbf{r})$, can then be written in the following way:

$$\psi(\mathbf{r}) = \sum_g \psi_g(\mathbf{r}) e^{2\pi i \mathbf{g}\cdot\mathbf{r}} \tag{2}$$

where $\mathbf{r}$ is in the *xy*-plane, conjugate with the image plane, and $\mathbf{g}$ the reciprocal lattice vectors of the perfect, or "reference", crystal [35]. Forward momentum is implicit and $\mathbf{g}$ also includes the transmitted beam. The imperfections of the crystal are treated entirely within the local Fourier components, $\psi_g(\mathbf{r})$, which have a local amplitude and phase:

$$\psi_g(\mathbf{r}) = a_g(\mathbf{r}) e^{i\phi_g(\mathbf{r})} \tag{3}$$

corresponding to the complex amplitudes of the transmitted and diffracted beams as a function of position across the exit surface of the crystal [36]. The phases here refer uniquely to the phases of Fourier components in reciprocal space and not those of the wave function in real space. We choose to write these phases as having four components:

$$\phi_g(\mathbf{r}) = \phi_g^G(\mathbf{r}) + \phi_g^C(\mathbf{r}) + \phi_g^M(\mathbf{r}) + \phi_g^E(\mathbf{r}) \tag{4}$$

where *C* refers to the crystalline lattice, *M* the magnetic contributions, *E* the electric fields and *G* the geometric phase [37]. This subdivision will always remain, to some extent, artificial since from a physical interaction standpoint, there are only two sources

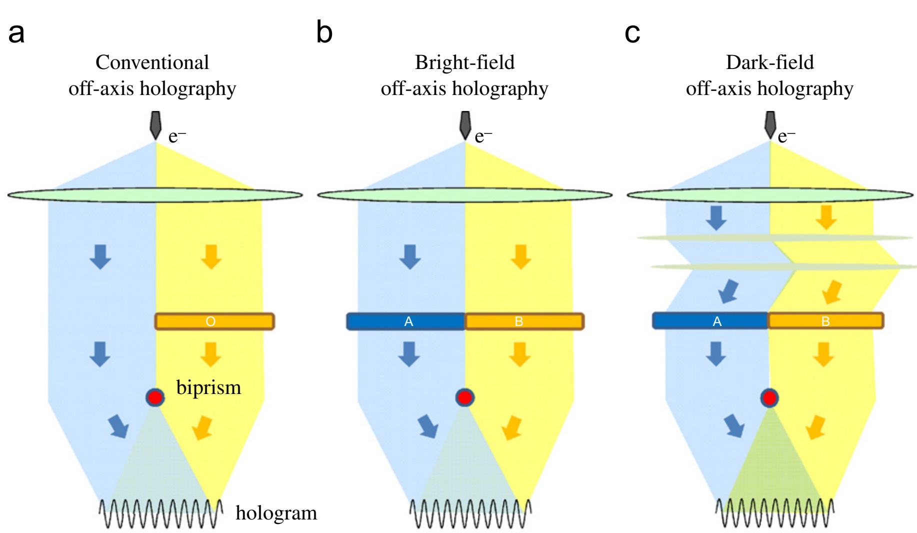

Fig. 1. Off-axis electron holography schemes: (a) conventional setup with specimen (O) and reference (vacuum); (b) bright-field holography with crystal (B) and reference crystal (A); (c) dark-field holography with strained crystal (B) and unstrained crystal (A).